Spatial Variability Analysis of Soil Physical Properties of Alluvial Soils

5 authors, including:

Javed Iqbal
COMSATS University Islamabad
11 PUBLICATIONS   **381** CITATIONS

J. Alex Thomasson
Texas A&M University
157 PUBLICATIONS   **1,573** CITATIONS

Johnie Jenkins
United States Department of Agriculture
394 PUBLICATIONS   **6,899** CITATIONS

Some of the authors of this publication are also working on these related projects:

Prior Publications View project

Cotton Disease Identification & Delineation Based on Remote Sensing View project

Spatial Variability Analysis of Soil Physical Properties of Alluvial Soils

Javed Iqbal,* John A. Thomasson, Johnie N. Jenkins, Phillip R. Owens, and Frank D. Whisler

ABSTRACT

Analysis and interpretation of spatial variability of soils is a keystone in site-specific farming. Soil survey maps may have up to 0.41-ha inclusions of dissimilar soils within a mapping unit. The objectives of this study were to determine the degree of spatial variability of soil physical properties and variance structure, and to model the sampling interval of alluvial floodplain soils. Soil profiles ($n = 209$) from 18 parallel transects were sampled with a mean separation distance of 79.4 m. Each profile was classified into surface, subsurface, and deep horizons. Structural analysis of soil bulk density (ρ_b), sand, clay, saturated hydraulic conductivity (K_s), volumetric water content (θ_v) at seven pressure potentials (Ψ_a) ($-1, -10, -33, -67, -100, -500,$ and -1500 kPa) were modeled for the three horizons. Variance of soil physical properties varied from as low as 0.01% (ρ_b) to as high as 1542% (K_s). The LSD test indicated significant ($P < 0.05$) differences in sand, clay, ρ_b, K_s, and θ_v at various Ψ_a. Geostatistical analyses illustrated that the spatially dependent stochastic component was predominant over the nugget effect. Structured semivariogram functions of each variable were used in generating fine-scale kriged contour maps. Overall autocorrelation, Moran's I, indicated a 400-m sampling range would be adequate for detection of spatial structure of sand, silt, clay, and a 100-m sampling range for soil hydraulic properties and ρ_b. The magnitude and spatial patterns soil physical property variability have implications for variable rate applications and design of soil sampling strategies in alluvial floodplain soils.

S PATIAL VARIABILITY of soil physical properties within or among agricultural fields is inherent in nature due to geologic and pedologic soil forming factors, but some of the variability may be induced by tillage and other management practices. These factors interact with each other across spatial and temporal scales, and are further modified locally by erosion and deposition processes. Soils in the Mississippi Delta are alluvial in nature, originating from different soils, rocks, and unconsolidated sediments in 24 states from Montana to Pennsylvania, and deposited by the Mississippi and Ohio Rivers and their tributaries (Logan, 1916). The stratification of different sediments deposited on top of each other spatially vary, for example, sandy sediments on top of clays or at other locations clay sediments depos-

ited on sandy or on loamy sediments. Therefore, it is important to study not only the extent of surface spatial variability, but also the distribution of subsurface and deep soil horizons.

Among the various soil physical properties, K_s and related measures are reported to have the highest statistical variability (Biggar and Nielsen, 1976). Bouma (1973) stressed the need for more studies on field variability of K_s and soil water retention curves. Stockton and Warrick (1971) indicated that variability in K_s is both a function of soil depth and position in the landscape, as well as experimental errors in measuring K_s. Cameron (1978) sampled clay loam soils at six depths from five grid-sampled locations in a 225-m^2 plot. He used the desorption method to determine soil water retention curves at pressure heads ranging from -10 to -500 kPa to calculate K_s. He found no consistent trend across sampling depths in pressure head values from -10 to -500 kPa, but the shape and magnitude of the average water retention curve differed among locations. He further reported that the coefficient of variation of soil water content ranged from 4.3 to 13% in the surface layer and from 2.4 to 6.5% in the deeper layers. In a study of spatial variability in soil hydraulic properties, Vieira et al. (1981) used variogram, kriging, and co-kriging techniques to determine the magnitude of spatial variation and reported a range of 50 m for 1280 field measured infiltration rates. Vauclin et al. (1983) sampled within a 70- by 40-m area at the nodes of a 10-m square grid and used classical and geostatistical techniques to study spatial variability of sand, silt, and clay contents, available water content (AWC), and water stored at -33 kPa. The strongest correlation was found between sand content and AWC ($r = -0.83$) and the cross variogram demonstrated that sand content was spatially correlated with soil water content at -33 kPa within a distance of $\approx$30 m and with AWC within a distance of $\approx$43 m. Sobieraj et al. (2003) found no spatial structure in K_s at distances > 25 m. Heiskanen and Makitalo (2002) reported a range of 44 and 100 m for the water content and air-filled porosity at $\Psi_a = -10$ kPa. Campbell (1978) reported sand content semivariogram ranges of 30 and 40 m for two different soil types. In summary, it is evident from the above studies that spatial variability of various soil physical properties are scale-dependent, especially the water transport properties of soils; therefore, it is a prerequisite to quantify the spatial variability of soils before designing site-specific applications like variable rate irrigation (VRI), seed rate, fertilizer rate, and strategies for future soil sampling, especially for alluvial floodplain soils. The objec-

Abbreviations: θ_v, volumetric water content; ρ_b, soil bulk density; Ψ_a, pressure potential; AWC, available water content; FC, field capacity; K_s, saturated hydraulic conductivity; OM, organic matter; VRI, variable rate irrigation; WP, wilting point.

tives of this study were to determine the degree of spatial variability of soil physical properties, variance structure, and model the sampling interval of alluvial floodplain soils.

MATERIALS AND METHODS

Soils of the Study Site

The study was conducted on a 162-ha cotton (*Gossypium* spp.) field near Perthshire (34°00′41′′ N, 90°55′39′′ W, with 2-m elevation range), MS. The field was irrigated by a center pivot system, and the major drainage areas were located on the east side of the field (Fig. 1). Major soil types included Commerce (fine-silty, mixed, superactive, nonacid, thermic Fluvaquentic Endoaquepts), Robinsonville (coarse-loamy, mixed, superactive, nonacid, thermic Typic Udifluvents), and Convent (coarse-silty, mixed, superactive, nonacid, thermic Fluvaquentic Endoaquepts).

Soil Sampling and Laboratory Analysis

The field was divided into 18 parallel transects (Fig. 1), and 209 soil profiles were sampled at a mean separation distance of 79.4 m. Because of the circular shape of the field, the number of sampling locations in each transect ranged from 5 to 14. Soil profiles were collected using a tractor-mounted Giddings no. 10-T Model GST hydraulic soil sampling and coring machine (Giddings Machine Co., Fort Collins, CO). The coordinates of each sampling location were recorded using a differential global positioning system unit. A stainless steel sampler tube was used to take a 1-m-deep soil profile. The soil profile was pushed from the sampler using a plunger into a polyvinyl chloride trough. This was done carefully so that the soil profile would not break. Using a knife and measuring tape, soil horizons were located and each horizon depth was recorded. A soil survey report (USDA-NRCS, 1951) of Bolivar County, Mississippi, was used to identify soil types. A soil sample from each horizon was placed into its designated bucket, mixed, and packed into boxes. Samples were air dried, crushed, sieved (2 mm), and analyzed for soil particle size distribution using the hydrometer method (Gee and Bauder, 1986) and organic C by the dry combustion method (Rabenhorst, 1988). Additional undisturbed soil cores were collected from surface, subsurface, and deep horizons using a Gidding sampler head containing 7.62- by 7.62-cm and 7.62- by 1-cm rings. These undisturbed samples were used for determination of ρ_b, K_s, and θ_v at seven Ψ_a (-1, -10, -33, -67, -100, -500, and -1500 kPa). The AWC was calculated as the difference between θ_v at -1500 kPa [permanent wilting point (WP)], -10 kPa [field capacity (FC) for light textured soils], and -33 kPa (FC for heavy textured soils) (Jury et al., 1991).
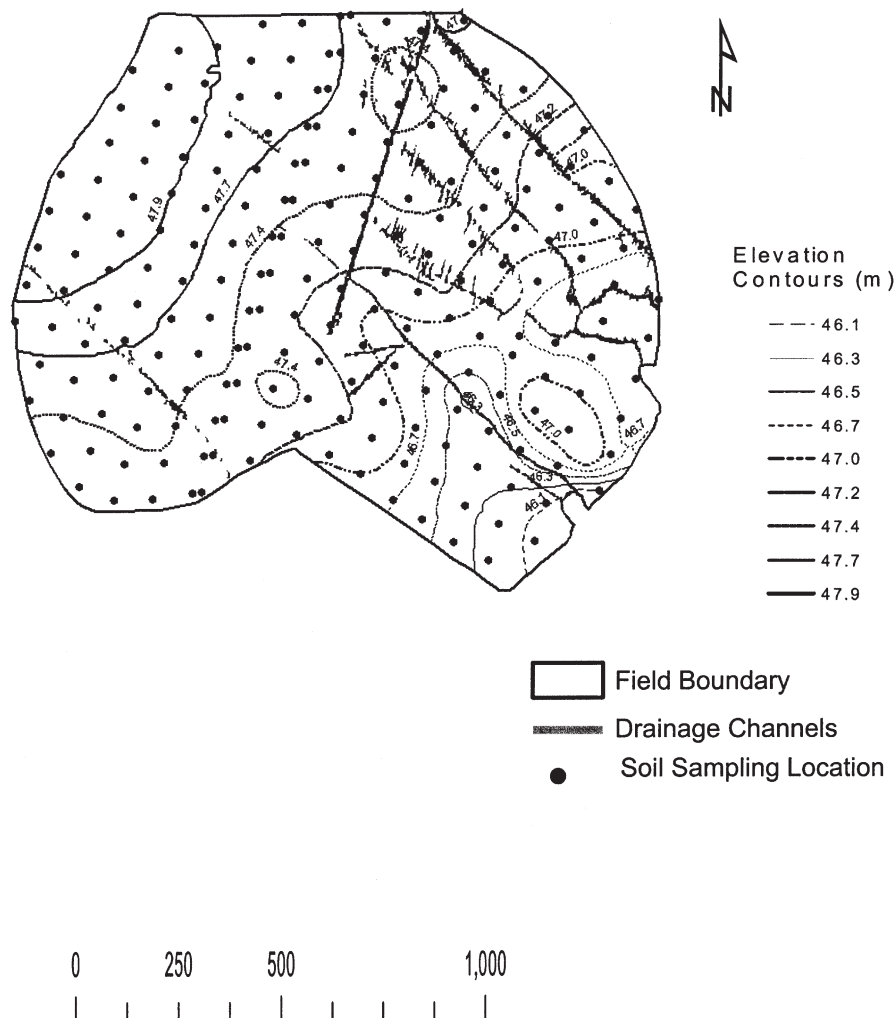
The pressure plate apparatus (Klute, 1986) was used to

Fig. 1. Map of study site showing 209 soil sampling locations, drainage channels, and elevation contours (m).

determine θ_v of 7.62- by 1-cm soil cores at seven Ψ_a (-1, -10, -33, -67, -100, -500, and -1500 kPa). First, the soil cores were saturated for 2 or 3 d at room temperature (24°C) and then weighed and placed on presoaked ceramic plates. A Ψ_a of -1 kPa was applied and maintained until equilibrium was achieved. Then soil cores were weighed and the same procedure was repeated for -10, -33, -67, -100, -500, and -1500 kPa. The θ_v at each Ψ_a was calculated on an oven-dry basis. For determination of K_s on each 7.62 × 7.62 cm soil core, a double layer of cheesecloth was secured to the bottom of the core with a rubber band, wax paper was laid over the top to prevent water evaporation, and the soil cores were placed in a shallow tray of water and allowed to saturate by equilibration for 2 or 3 d at room temperature. Once saturated, the K_s for each soil core was determined using the falling head method (Klute and Dirksen, 1986).

Statistical Methods

Measured variables in the data set were analyzed using classical statistical methods to obtain the minimum, maximum, mean, median, skewness (Shapiro and Wilk, 1965), and standard deviation at each horizon ($n = 209$). A one-way ANOVA was also performed (SAS Institute, 1996) to compare each variable across the soil profile using a protected least significant ($P < 0.05$) difference test (Table 1). The Shapiro-Wilk test revealed that all measured variables were skewed significantly ($P > 0.05$) except for ρ_b of the surface horizons and organic matter (OM) of the subsurface horizons. Skewed variables were transformed either using natural logarithm or square root methods to a nearly normal distribution before using geostatistical analysis; then, the data were back transformed using a weighted technique. A weighted technique is considered superior to a simple back transformation because it more closely approximates true population statistics (Haan, 1997).

The degree of spatial variability for each variable was determined by geostatistical methods using semivariogram analysis, kriging, and autocorrelation (Trangmar et al., 1985; Bailey

and Gatrell, 1998; McBratney and Pringle, 1999). Before applying the geostatistical tests, each variable was checked for normality, trend, and anisotropy. A geographic trend was determined using exploratory data analysis tools in S+ SpatialStats (S-Plus, 1997). If a variable had a geographic trend, then a first-order (linear) model was developed between soil variable z (dependent variable) and the x, y geographic coordinates (independent variables). The linear trend model was tested as an ordinary regression by ANOVA. If the linear trend model was significant ($P < 0.05$), then the soil variable was detrended by subtracting the soil variable values from the linear model calculations. The residuals were regarded as closer to stationary and were used to calculate semivariograms. The residual interpolation was performed with ordinary kriging. Finally, adding the kriged residuals to the first order trend completed the mapping of the variate.

Since the exact form of semivariogram model was never known, the given model selected and used was only an approximation of its function (Journel and Huijbregts, 1978). However, to come up with a best model, a jack-knifing procedure was performed. In this trial-and-error method, every known point was estimated using the surrounding data points but not the measured data point. Thus, every semivariogram for each soil variable was adjusted by trial and error until a best fit between the estimated and actual values was found (Bailey and Gatrell, 1998).

A semivariogram was determined for each variable to ascertain the degree of spatial variability between neighboring observations, and the appropriate model function was fit to the semivariogram. The semivariogram function (Goovaerts, 1997) was calculated as follows:

$$\gamma(h) = \frac{1}{2N(h)}\left\{\sum_{i=1}^{N(h)}[Z(x_i + h) - Z(x_i)]^2\right\} \quad [1]$$

where (h) is the semivariance for interval class h, $N(h)$ is the number of pairs separated by lag distance (separation distance between sample positions), $Z(x_i)$ is a measured variable at

Table 1. Descriptive statistics for selected soil physical properties ($n = 209$) for surface, subsurface, and deep soil horizons.

Variable†	Horizon	Min.	Max.	Mean‡	Median	Skewness§	SD
ρ_b, g cm^{-3}	surface	0.90	1.41	1.21b	1.21	-0.23	0.09
	subsurface	0.98	1.49	1.28a	1.29	-0.43	0.10
	deep	0.80	1.49	1.20b	1.20	-0.46	0.11
K_s, cm d^{-1}	surface	0.03	283.75	24.46a	9.62	3.54	39.28
	subsurface	0.03	63.47	6.03c	2.31	2.96	9.33
	deep	0.05	153.86	12.44b	4.67	3.62	21.49
Sand, %	surface	1.09	74.56	27.69a	25.48	0.53	19.15
	subsurface	0.78	85.87	24.40a	19.64	0.76	20.68
	deep	0.27	91.36	28.28a	24.53	0.46	23.21
Clay, %	surface	5.00	33.85	11.32c	10.10	1.06	7.34
	subsurface	0.63	45.97	14.88a	12.76	0.86	9.57
	deep	0.63	53.30	13.18b	10.87	1.22	10.21
Silt, %	surface	16.02	95.07	60.99a	64.91	-0.52	16.62
	subsurface	12.87	95.97	60.72a	63.86	-0.53	16.73
	deep	7.38	97.15	58.54a	59.13	-0.09	20.11
OM, %	surface	0.42	2.32	1.162a	1.13	0.32	0.39
	subsurface	0.30	2.02	0.93b	0.90	0.32	0.34
	deep	0.00	1.84	0.93b	0.90	0.32	0.33
FC, cm^3 cm^{-3}, %	surface	11.58	43.97	28.35c	29.43	-0.31	6.67
	subsurface	12.50	49.39	29.84b	30.79	-0.22	7.33
	deep	10.37	56.80	31.92a	33.18	-0.28	8.91
WP, cm^3 cm^{-3}, %	surface	5.07	35.35	16.79c	16.88	0.30	5.93
	subsurface	6.14	43.75	20.26b	20.78	0.16	7.81
	deep	4.41	43.33	22.76a	23.20	-0.05	8.97
AWC, cm^3 cm^{-3}, %	surface	4.74	26.92	11.56a	11.10	0.99	3.50
	subsurface	4.30	18.53	9.58b	9.16	0.76	2.74
	deep	4.07	24.74	9.27b	8.75	1.38	3.14

† AWC = available water content, calculated as the difference between -10, -33, and -1500 kPa; FC = field capacity, volumetric water content at -10 and -33 kPa; K_s = saturated hydraulic conductivity; OM = organic matter; WP = wilting point, volumetric water content at -1500 kPa.

‡ Means for each variable followed by the same letter are not significantly different by LSD test at $P < 0.05$.

§ Shapiro-Wilk test was used to test the significance level of normality, all variables were significantly ($P > 0.05$) skewed, except ρ_b at surface and OM at deep horizons.

spatial location i, $Z(x_i + h)$ is a measured variable at spatial location $i + h$. A semivariogram consists of three basic parameters which describe the spatial structure as: $\gamma(h) = C_o + C$. C_o represents the *nugget effect*, which is the local variation occurring at scales finer than the sampling interval, such as sampling error, fine-scale spatial variability, and measurement error; $C_o + C$ is the *sill* (total variance); and the distance at which semivariogram levels off at the sill is called the *range* (beyond that distance the sampling variables are not correlated).

We created contour maps of each variable at each horizon through ordinary kriging (David, 1977; Journel and Huijbregts, 1978; and Clark, 1979) using their respective semivariogram models in S+ SpatialStats (S-Plus, 1997).

Sampling Interval

Spatial Autocorrelation

Autocorrelation has been used to express spatial changes in field-measured soil properties and the degree of dependencies among neighboring observations. Such information aids in identifying the adequate soil sampling interval for which observations remain spatially correlated and can be used for designing soil-sampling schemes (Webster, 1973; Webster and Cuanalo, 1975; Gajem et al., 1981; Vieira et al., 1981).

The spatial autocorrelation, Moran's I statistics (Moran, 1950), was used to calculate the coefficient at selected lag distances. Moran's I is a measure of autocorrelation similar in interpretation to the Pearson's correlation statistics, and both statistics range from +1.0 meaning strong positive spatial autocorrelation, to 0 meaning a random pattern, to −1.0 indicating strong negative spatial autocorrelation. The statistic for Moran's I is defined as:

$$I = \left[\frac{n}{\sum_{i=1}^{n}\sum_{j=1}^{n} w_{ij}} \right] \left[\frac{\sum_{i=1}^{n}\sum_{j=1}^{n} w_{ij}(x_i - \bar{x})(x_j - \bar{x})}{\sum_{i=1}^{n}(x_i - \bar{x})^2} \right] \quad [2]$$

Where n is the number of points, x the variable of interest,

$\bar{x}$ the mean of x, and w_{ij} the spatial weight describing the adjacency or distance between the ith and jth point. The significance of the Moran's I coefficient at successive lags were evaluated under the randomization hypothesis (Cliff and Ord, 1973).

RESULTS AND DISCUSSION

Variation among Soil Horizons

Values for ρ_b in the subsurface horizon were significantly ($P < 0.05$) greater than in the surface and deep horizons (Table 1). Increased ρ_b and very low values for K_s mean (6.03 cm d^{-1}) and range (0.03–63.47 cm d^{-1}) in subsurface horizons indicate downward movement of water is restricted by a compacted subsurface layer observed at about 31- to 62-cm depth. This may be due to compaction of fine sandy or fine silt layers by the usage of heavy machinery on the farm and monoculture (cotton).

The K_s of all surface horizons was on average about two times greater than for deep horizons, and four times greater than all subsurface horizons. Increased K_s values in surface horizons could be due to lower ρ_b owing to the presence of root channels and macroporosities. Similar conclusions was reported by Rasse et al. (2000), who found alfalfa root systems increased water flow, as indicated by higher K_s, total and macroporosities, and water recharge rates of the Ap horizon. Increases in K_s appeared to have resulted from greater macroporosities. Rasse et al. (2000) attributed those results to increased amplitudes of wetting and drying cycles and higher rates of root turnover in the Ap horizon. No significant ($P > 0.05$) differences were found in the mean sand and silt content of the three horizons. While OM contents differ significantly ($P < 0.05$) between the three horizons, the θ_v at FC and at WP increased significantly ($P < 0.05$)

Table 2. Semivariogram parameters of soil physical properties.

Variable†	Horizon	Model‡	Nugget	Sill	Nugget¶	Spatial class	Range	R	Cross validation R
					%		m		
$\rho_{b,\, g\, cm^{-3}}$	surface	Exp.	0.002	0.007	29	M	106	0.92	0.346
	subsurface	Exp.	0.003	0.009	33	M	107	0.78	0.339
	deep	Exp.	0.006	0.017	35	M	132	0.96	0.338
K_s, cm d^{-1}	surface	Exp.	0.460	1.506	31	M	94	0.96	0.376
	subsurface	Exp.	0.455	0.917	50	M	110	0.87	0.339
	deep	Exp.	0.590	2.190	27	M	111	0.77	0.551
Sand, %	surface	Exp.	78	427	18	S	421	0.99	0.790
	subsurface	Exp.	155	452	34	M	238	0.98	0.681
	deep	Exp.	151	520	29	M	137	0.99	0.660
Clay, %	surface	Exp.	16	65	25	M	218	0.98	0.710
	subsurface	Exp.	32	95	34	M	139	0.99	0.701
	deep	Exp.	54	108	50	M	144	0.99	0.542
FC, cm³ cm⁻³, %	surface	Sph.	16	60	27	M	741	0.99	0.729
	subsurface	Sph.	18	76	23	S	861	0.99	0.688
	deep	Sph.	33	102	32	M	997	0.99	0.637
WP, cm³ cm⁻³, %	surface	Sph.	12	70	18	S	425	0.99	0.640
	subsurface	Sph.	22	70	31	M	425	0.99	0.665
	deep	Sph.	21	77	28	M	153	0.98	0.588
AWC, cm³ cm⁻³, %	surface	Exp.	4	12	31	M	93	0.94	0.370
	subsurface	Exp.	2	7	22	S	99	0.97	0.434
	deep	Exp.	2	7	30	M	78	0.94	0.266

† AWC = available water content, calculated as the difference between −10, −33, and −1500 kPa; FC = field capacity, volumetric water content at −10 and −33 kPa; K_s = saturated hydraulic conductivity; OM = organic matter; WP = wilting point, volumetric water content at −1500 kPa.

‡ Exp. = Exponential; Sph. = spherical.

¶ % nugget = (nugget semivariance/total semivariance) × 100; S = strong spatial dependence (% nugget < 25); M = moderate spatial dependence (% nugget between 25 and 75).

as sampling depth increased among the three horizons. Comparatively low θ_v at WP in surface horizons resulted in AWC averaging from about 2.0 cm³ cm⁻³ (%) greater capacity in the surface than in the subsurface and deep horizons. The higher AWC in the surface horizons could be due to higher OM contents in the surface (1.2%) than deeper horizons (≈0.93%). The difference in AWC could be due to the cotton crop roots and shoots contributing more fresh OM inputs into the surface horizons, which promotes soil aggregation (Angers and Caron, 1998).

Spatial Structure Analysis

Table 2 presents the semivariogram parameters for selected variables for each horizon. We adopted spatial class ratios similar to those presented by Cambardella et al. (1994) to define distinctive classes of spatial dependence. If the ratio of spatial class was <25%, the variable was considered strongly spatially dependent; if the ratio was >25% and <75%, the variable was considered moderately spatially dependent; and if the ratio was >75%, the variable was considered weakly spatially dependent.
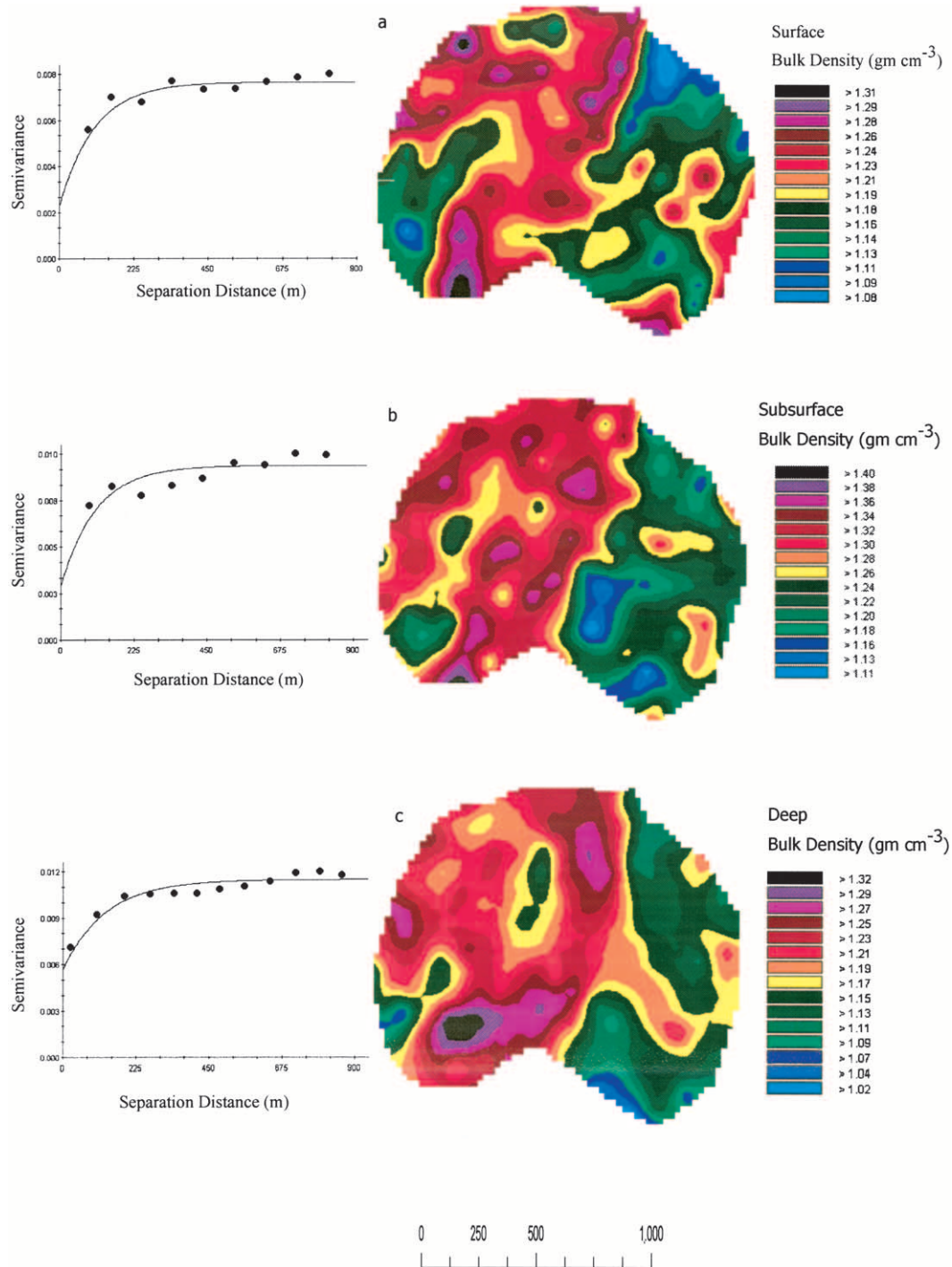

Fig. 2. Semivariograms and kriged maps of soil bulk density for the (a) surface, (b) subsurface, and (c) deep horizons.

The resulting semivariograms indicated the existence of moderate to strong spatial dependence for all soil physical properties for each horizon (Table 2). For example, with the exception of AWC in the subsurface horizons, the range of various semivariogram models which exceeded 79.4 m indicated the presence of spatial structure beyond the original average sampling distance.

Spatial structure analysis indicated spatial variability across field for soil texture, ρ_b, water retention, and K_s. With regard to ρ_b, the values for nugget, sill, % nugget, and range increased from the surface to the deep horizon. This increase indicated higher structured variance, nugget effect/random variability, and range with increase in depth, which may indicate a depositional event or a series of depositional events. Compared with the present study, Tsegaye and Hill (1998) observed lower structural variability in surface ρ_b, as judged from a higher nugget (0.003) and lower sill (0.004), that is, percentage nugget attributed 75% of total variability with a range value of 22 m. The lower range reported by Tsegaye and Hill (1998) could be due to a much smaller sampling interval of 1 m in a relatively small area (45 by 37 m) located on a level landscape. The semivariogram functions for K_s were exponential for the three horizons. In the surface horizon, we found somewhat lower nugget (0.46), sill (1.50), and percentage nugget (30.54), and higher range (94 m), as compared with values reported by Tsegaye and Hill (1998). However, the highest K_s nugget effect (50%) was found for the subsurface horizon, which may be due to the highest ρ_b values. While Bosch and
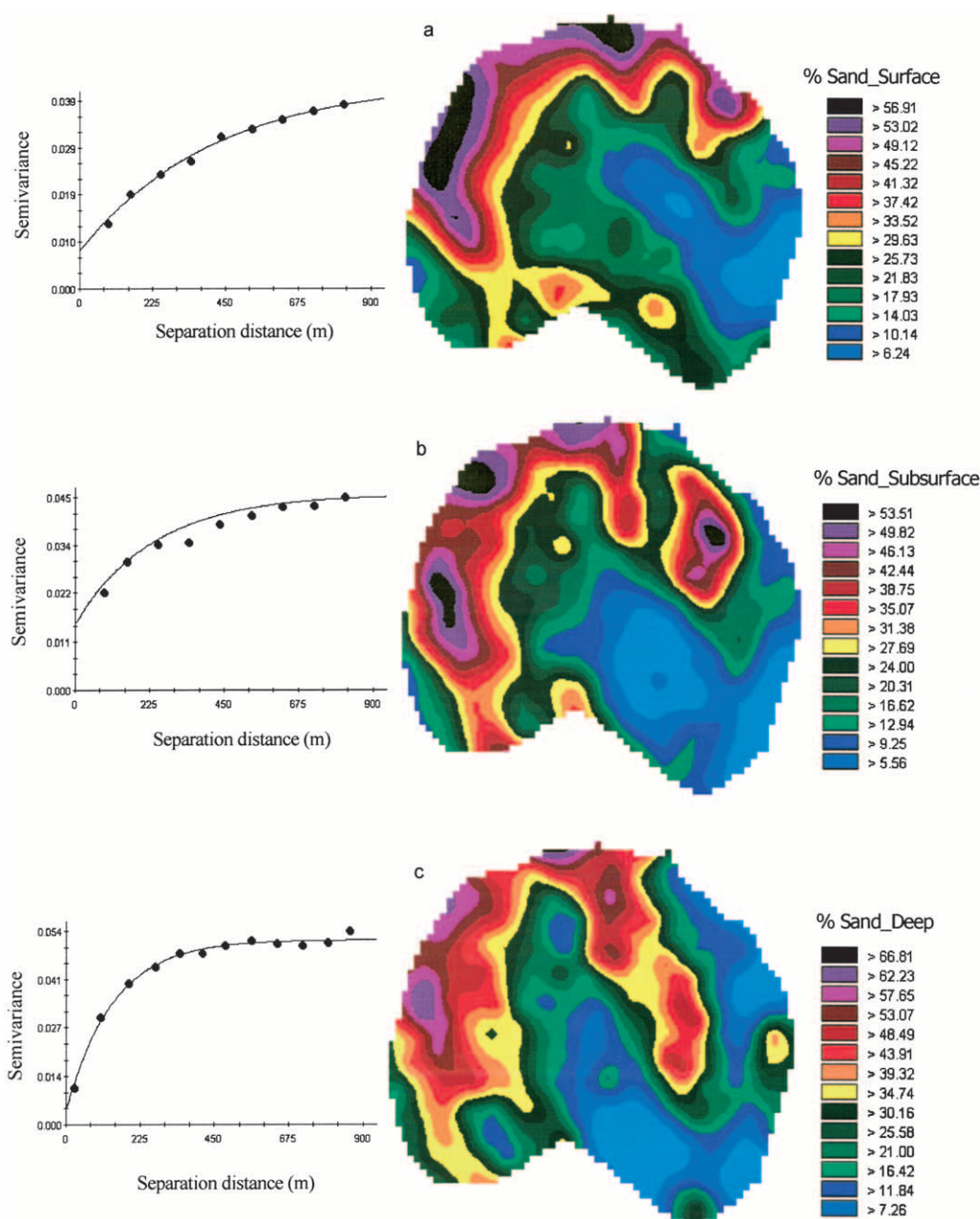

Fig. 3. Semivariograms and kriged maps of percentage sand content for the (a) surface, (b) subsurface, and (c) deep horizons.
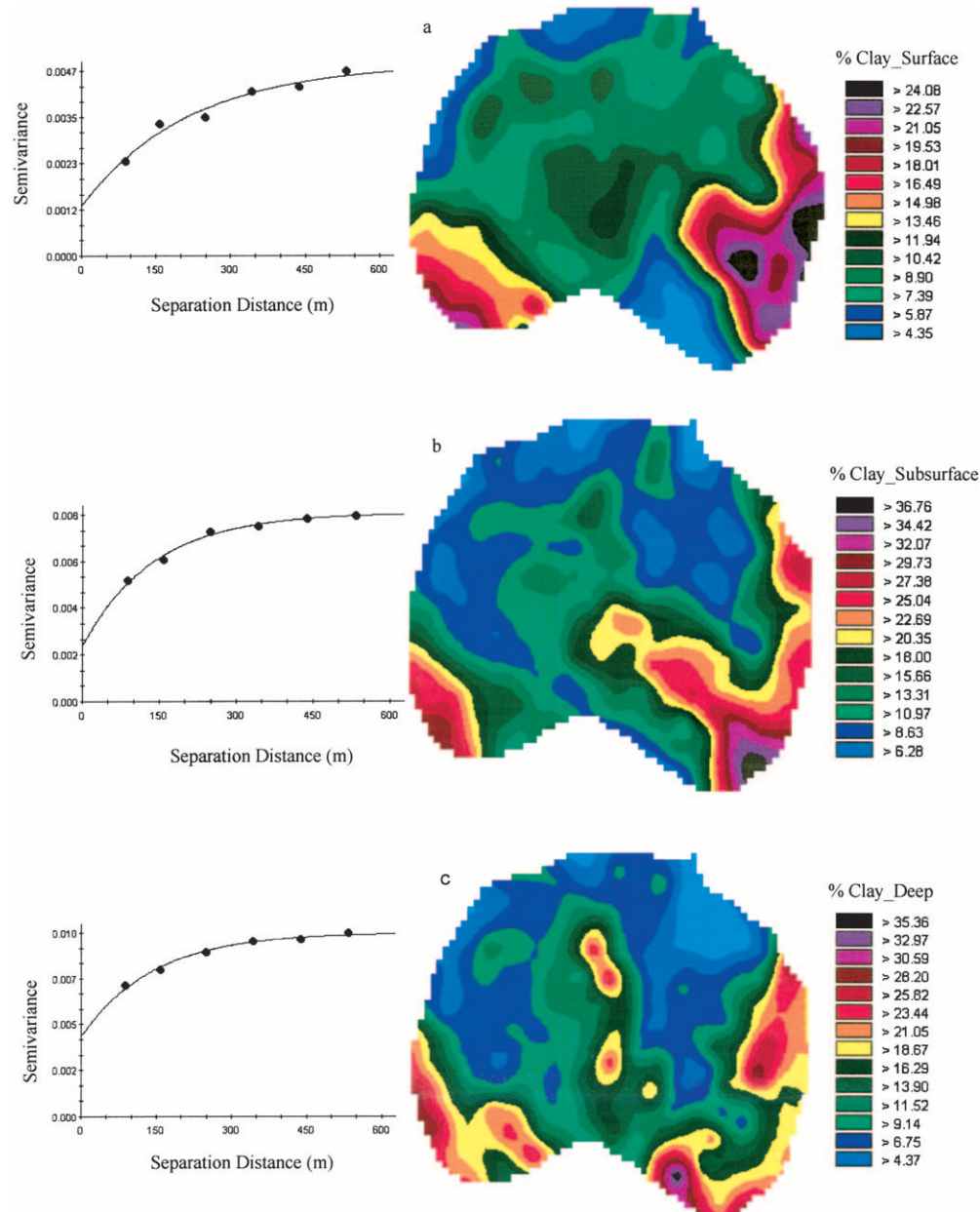
Fig. 4. Semivariograms and kriged maps of percentage clay content for the (a) surface, (b) subsurface, and (c) deep horizons.

West (1998) also reported the highest nugget effect of 95% for the subsurface (0.25–0.50 m) horizon as compared with surface and deep horizons. The semivariograms for sand and clay content revealed moderate to strong spatial structures for all three horizons. Higher percentage nugget effect with the lower range values for sand and clay content were found in the subsoil and deep soil horizons. These data may indicate the combined influence of surface tillage and stratification of different sediments at different spatial scales. Although studies of Vauclin et al. (1983) reported somewhat lower values for sill, nugget, and range in percentage sand content; they sampled a single soil type at 10-m intervals in a much smaller area (70 by 40 m). By contrast, we have encountered four soil types across a 162-ha field. With regard to water content at FC, semivariogram models indicated strong spherical structure in subsurface horizons, but moderate spherical

structure in the surface and deep horizons (Table 2). The range of influence of spatial structure in FC increased as depth increased from ≈741 m in the surface horizon to ≈997 m in deep horizons. The semivariograms for water content at WP indicated somewhat stronger spatial structure in the surface horizon than in the subsurface and deep horizons. Semivariograms for AWC were exponential, and this variable showed a strong spatial structure in subsurface horizon and moderate spatial structure in the surface and deep horizons. The range of influence of AWC was similar to the original 79.4 m, which is somewhat shorter than the ranges of water content at either WP or FC.

Contour Maps

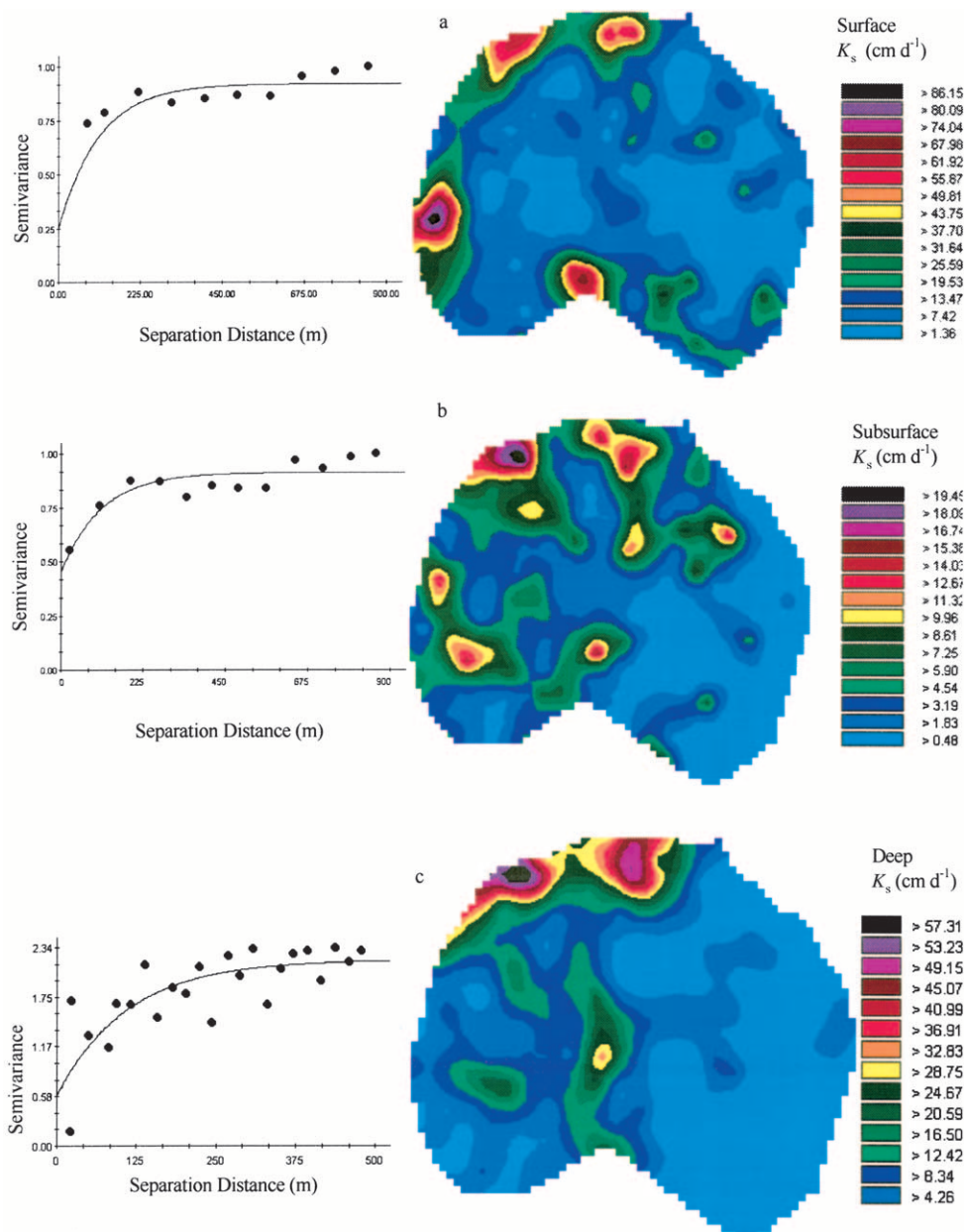Kriged contour maps indicated soils with high ρ_b in surface, subsurface, and deep horizons were found in

Fig. 5. Semivariograms and kriged maps of saturated hydraulic conductivity (K_s) for the (a) surface, (b) subsurface, and (c) deep horizons.

the western part of the field, extending mainly from SW to NW (Fig. 2). Soil profiles in these areas were classified as Robinsonville soil types, which are comprised of sandy to sandy loam soils. As expected, a significant ($P <$ 0.05) Pearson correlation was obtained between sand content and ρ_b in each horizon. The largest correlation was obtained in the subsurface horizon ($r = 0.35$), which typically had the highest ρ_b values (Table 1), an association that may be the result of heavy equipment usage on the field year-round, which would cause compaction in the fine sandy layer. Similar to kriged contour maps of ρ_b, soils with high sand content in the surface, subsurface, and deep horizons were found in the western part of the field extending from the NW quadrant to the SW quadrant (Fig. 3). Soils with low sand content were found in the southeastern part of the field, especially in the natural drainage areas (Fig. 1). A significant ($P <$

0.05) negative Pearson correlation 0.65 to 0.5 was obtained between sand and clay content in each horizon. Consequently, soils with low clay content in the surface, subsurface, and deep horizons were found in the western part of the field; whereas, higher clay contents were found in the eastern part of the field, especially in the natural drainage areas (Fig. 4). As expected, values for K_s in each horizon were positively associated with sand content and negatively associated with clay content. The kriged contour maps of K_s for the surface, subsurface, and deep horizons are depicted in Fig. 5. These maps for the surface and subsurface horizons show strong positional similarity with maps for clay content (Fig. 4), and lesser similarity to maps of sand content (Fig. 3). Kriged maps of the subsurface horizon illustrate positional similarity between sand, clay, and K_s mostly along the field east and west border, with less obvious or more
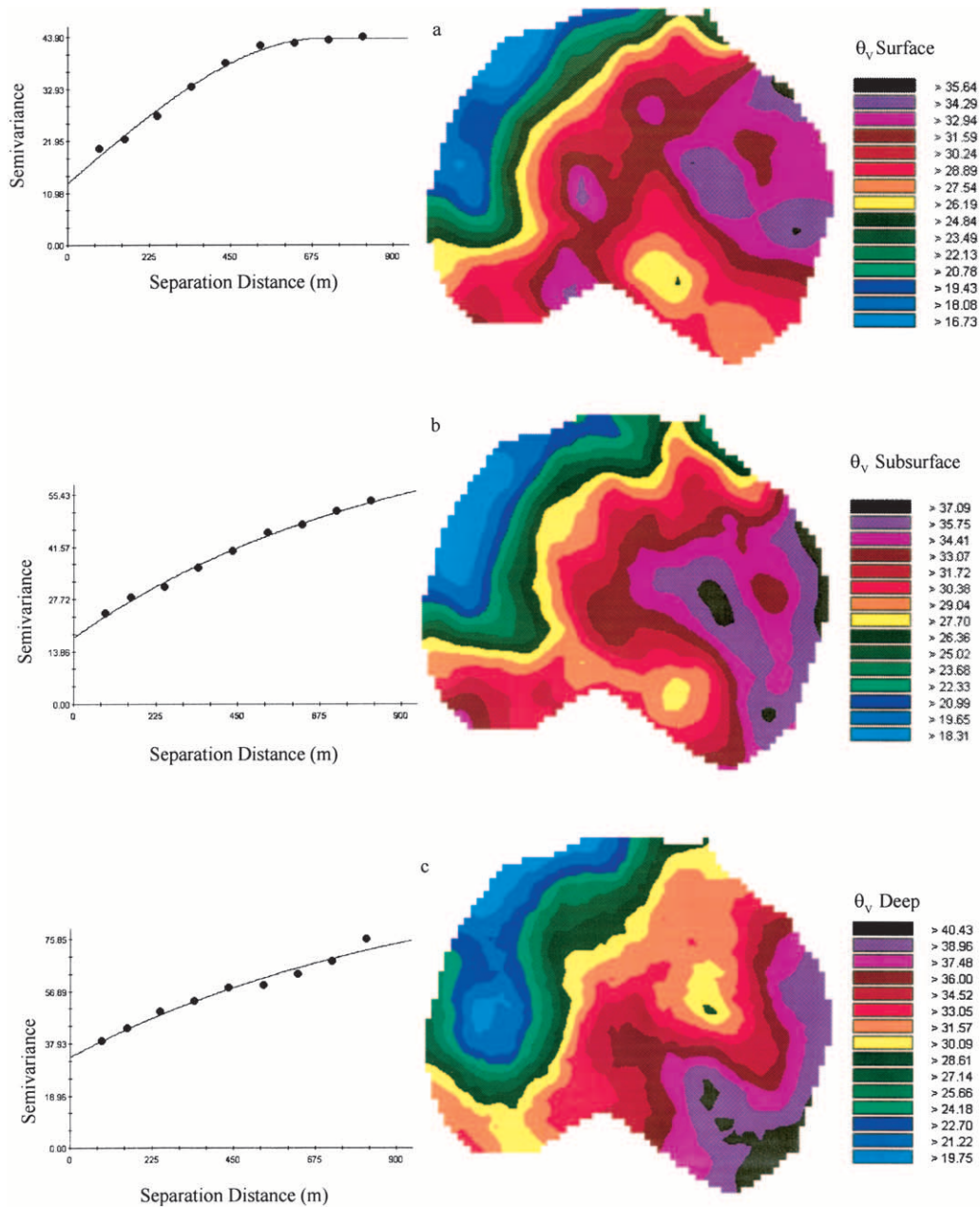
Fig. 6. Semivariograms and kriged maps of volumetric water content (θ_v), cm^3 cm^{-3}, expressed in percentage at field capacity (equivalent to -33 kPa pressure head) for the (a) surface, (b) subsurface, and (c) deep horizons.

complex positional effects evident in the field's interior. Soils with the highest K_s values in the subsurface were found along the NW edge of the field. Contour maps of sand content had the best positional similarity with kriged maps of θ_v at FC, WP, and AWC for the surface, subsurface, and deep horizons (Fig. 6, 7, 8). All of these maps indicated that soils in the western one-third of the field typically have low water retention at FC and WP, as well as lower AWC in each horizon.

In summary, the fine-scale distribution of various soil physical properties across the field have implications for variable rate application of fertilizer, water, seed rate, and so forth. For instance, the spatial distribution of water retention properties closely followed the distribution pattern of sand and clay content. This indicates a

differential water holding capacity of different textured soils across the field. Currently, the farmer uses a uniform application rate of 2 to 4 cm of water during the cotton growing season irrespective of different soil textures found across the field, which leads to the over- and underapplication of water in different parts of the field. This practice induced spatial variability in cotton lint yield, which varied from 280 to 1680 kg ha^{-1}, with a mean yield of 1092 $\pm$ 212 kg ha^{-1} during the 2002 growing season. The variability in cotton lint yield could be exploited by developing a VRI plan for the field. The VRI plan could be implemented by combining spatial variability maps of sand and clay content of a given field into the soil texture map. The fine scale soil texture map could be used as a base map for developing a
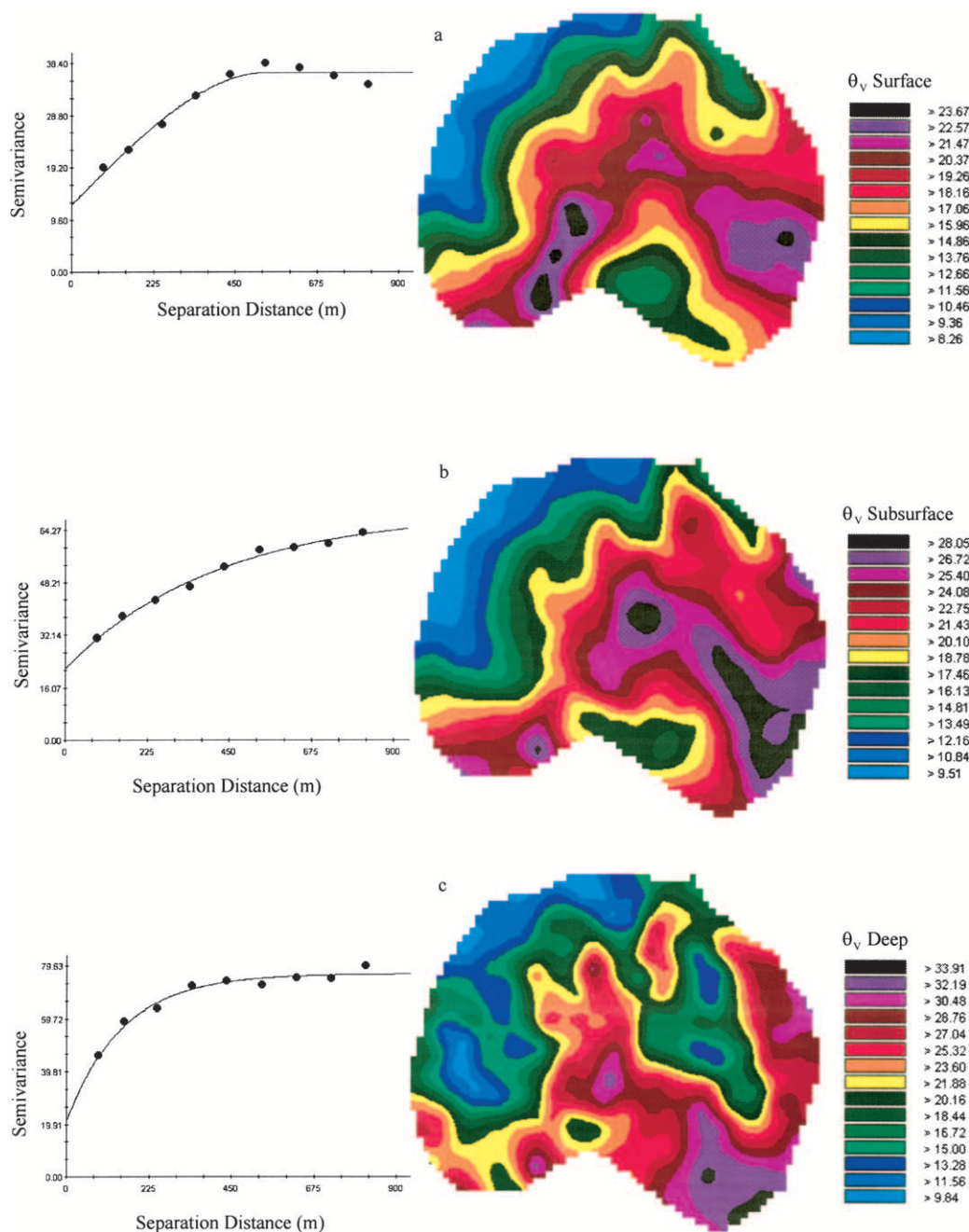
Fig. 7. Semivariograms and kriged maps of volumetric water content (θ_v), cm^3 cm^{-3}, expressed in percentage at wilting point (equivalent to -1500 kPa pressure head) for the (a) surface, (b) subsurface, and (c) deep horizons.

prescription map for VRI. The VRI plan for the field would not only optimize yield by avoiding crop water stress in highly prone areas, but would also reduce groundwater and surface water N pollution due to over-irrigation resulting in runoff and percolation.

Spatial Autocorrelation

The soil physical property correlograms exhibited a degree of smoothness, and was reflected in a positive spatial autocorrelation structure with no apparent cyclicity (Fig. 9). The autocorrelation at zero lag is 1, and it begins to decline as the lag distance increases and eventually decreases to an insignificant level at a lag

distance of 900 m. In general, soil ρ_b and hydraulic properties revealed significant ($P < 0.05$) autocorrelation only at shorter lag distances compared with the percentage sand, silt, and clay contents for the three horizons. In addition, different horizons of the same soil physical property exhibited different sampling extent of spatial autocorrelation, Moran's I ($P < 0.05$) values.

Correlograms of soil ρ_b showed significant Moran's I at lag distance of 100 m for surface and deep horizons and 300 m for subsurface horizons. Sand and silt content had a similar pattern of spatial autocorrelation extent for the three horizons: that is, each soil property showed a significant Moran's I at 600 m for the surface and
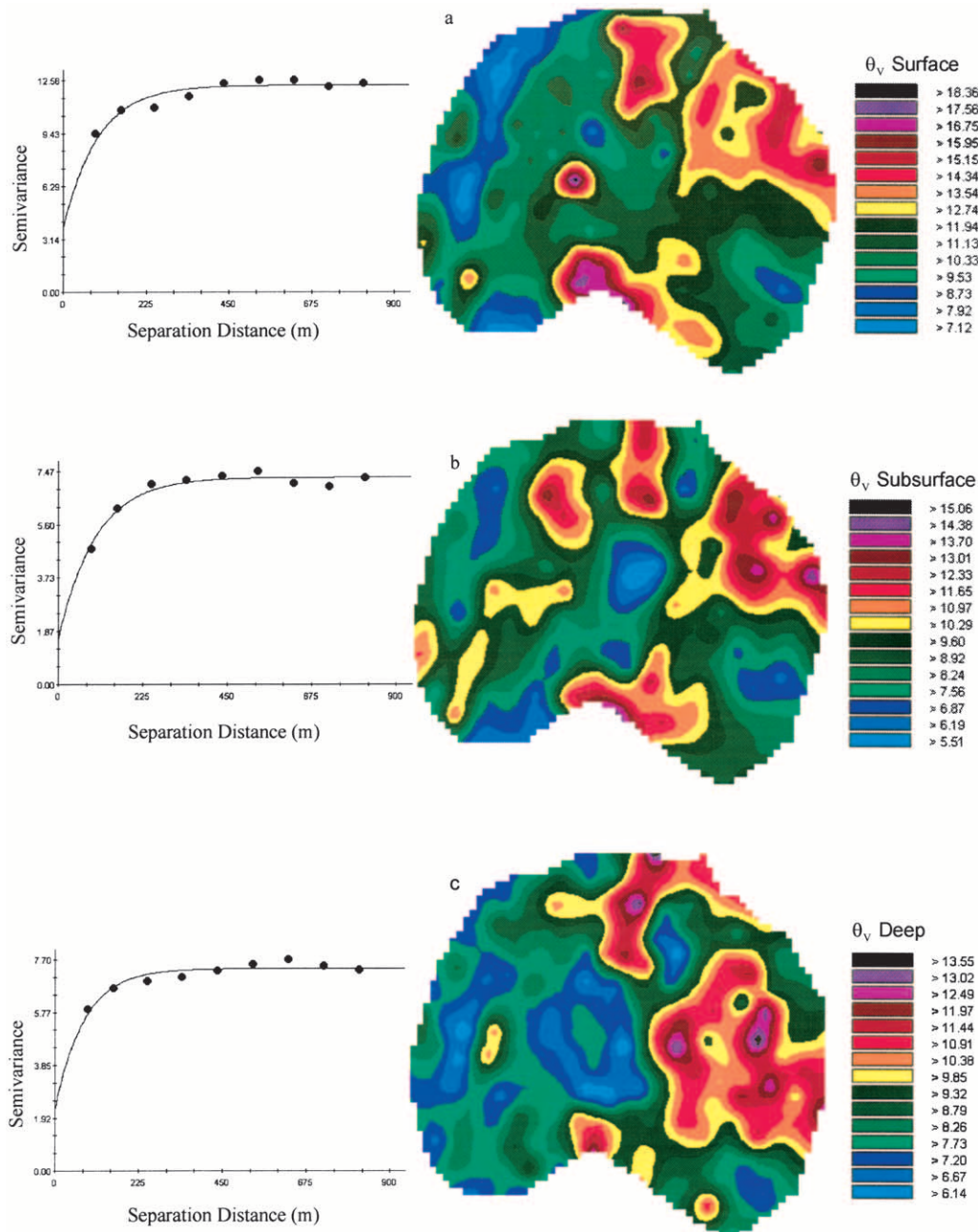
Fig. 8. Semivariograms and kriged maps of available water content (AWC), cm³ cm⁻³, expressed in percentage for the (a) surface, (b) subsurface, and (c) deep horizons.

400 m for the subsurface and deep horizons. However, the clay content correlogram had a significant Moran's *I* at 400 m for surface and subsurface horizons and 300 m for deep horizons. Soils in the Mississippi Delta, especially along the Mississippi River, are minimally developed Entisols showing little evidence of pedogensis, and diagnostic surface and subsurface horizons are typically absent; therefore, differences in the particle size and its spatial autocorrelation extent are not likely related to pedogenic processes, such as eluviation and illuviation. These alluvial floodplain soils have different stratification extents for the same soil physical property at different horizons. This suggests that the degree of cumulization and the extent of stratification during de-

position of the alluvial materials is the most important factor in explaining the significant extent of spatial autocorrelation, Moran's *I* differences at surface, subsurface, and deep horizons. Those differences and anthropogenic activities, like subsoiling, affected the spatial autocorrelation of soil hydraulic properties in the surface and subsurface horizons. The correlograms of K_s and θ_v at −1500 kPa had a significant ($P = 0.05$) Moran's *I* at 100 m for three horizons; however, K_s showed stronger autocorrelation for deep horizons when compared with the surface and subsurface horizons. The correlograms of θ_v at −10 kPa Ψ_a showed a weakly significant ($P < 0.1$) autocorrelation, Moran's *I* at 100 m at surface horizon but a stronger and significant ($P <$
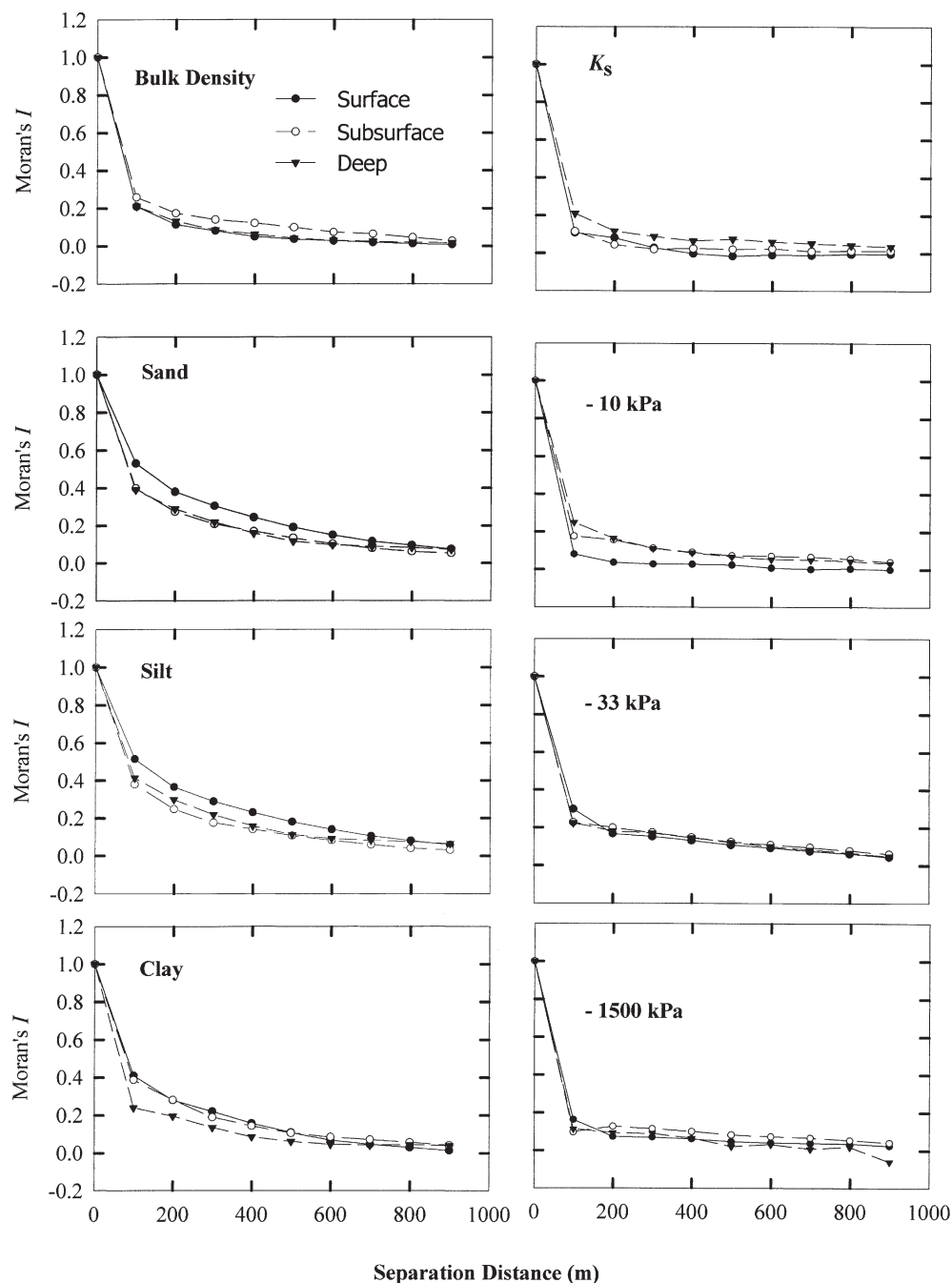
Fig. 9. Spatial autocorrelation, Moran's *I*, of soil physical properties for surface, subsurface, and deep soil horizons (*n* = 209). *K*$_s$ is saturated hydraulic conductivity (cm d^{-1}), and values −10, −33, and −1500 kPa represent volumetric water content (cm^3 cm^{-3}, expressed as a percentage) at specified pressure head.

0.05) Moran's *I* at 200 m for subsurface and deep horizons. The correlograms of θ$_v$ at −33 kPa Ψ$_a$ showed significant (*P* < 0.05) Moran's *I* values at 300 m for the surface and 400 m for the subsurface and deep horizons.

In summary, the autocorrelation between sampling points weakened steadily across distances from 100 to 900 m. On the basis of Moran's *I* (*P* < 0.05) for each soil physical property, sampling at spacing closer than 400 m for soil texture, and closer than 100 m for soil hydraulic properties and ρ$_b$ would be needed to detect boundaries of these soil properties in alluvial floodplain soils of Mississippi Delta.

SUMMARY

The classical and geostatistical methods revealed statistical and spatial variability in soil physical properties among soil horizons and across the field. Values for ρ$_b$ in the subsurface horizon were significantly (*P* < 0.05) greater than in the surface and deep horizons. Increased ρ$_b$ and very low values for *K*$_s$ mean (6.03 cm d^{-1}) and range (0.03–63.47 cm d^{-1}) in subsurface horizons indicate downward movement of water is restricted by a compacted subsurface layer observed at about the 31- to 62-cm depth. This may be because of compaction of

fine sandy or fine silty layers by the usage of heavy machinery. Mean soil OM and AWC displayed a small but steadily decreasing trend from the surface horizon to the deeper horizons.

Semivariogram spatial structures of different soil physical properties revealed that structured variance was dominant over nugget effect/random component. The percentage nugget values ranged from 18 to 50, that is, lowest for sand and θ_v at WP in surface horizons and highest for surface K_s. Kriged contour maps of various soil physical properties showed moderate to strong positional similarities. For example, the area of the field with higher sand content had higher K_s values, lower clay content, and lower corresponding values of θ_v at FC, WP, and AWC. These spatial variability maps of various soil physical properties have implications for site-specific farming, for example variable-rate irrigation, N-fertilizer application, and seed rate. In a variable-rate fertilizer-N and water application study, Mckinion et al. (2001) used soil physical properties data collected in this research in a site-specific cotton crop simulation (GOSSYM/COMAX-GIS integrated) to optimize cotton lint yield. The model simulation results showed that an increase of 322 kg ha^{-1} cotton lint yield could be achieved by an overall increase of 2.6 cm ha^{-1} water application and a decrease of 35 kg N ha^{-1} fertilizer.

Autocorrelation, Moran's I statistics was used to investigate the adequate sampling interval for various soil physical properties. All the correlograms show positive spatial autocorrelation without any cyclicity. The Moran's I values indicated that sampling at spacing closer than 400 m for soil texture and less than 100 m for soil hydraulic properties and ρ_b would be needed for designing soil sampling in the floodplain of Mississippi Delta.

REFERENCES

Angers, D.A., and J. Caron. 1998. Plant-induced changes in soil structure: Processes and feedbacks. Biogeochemistry 42:55–72.
Bailey, T.C., and A.C. Gatrell. 1998. Interactive spatial data analysis. Addison Wesley Longman, UK.
Biggar, J.W., and D.R. Nielsen. 1976. Spatial variability of leaching characteristics of a field soil. Water Resour. Res. 12:78–84.
Bouma, J. 1973. Use of physical methods to expand soil survey interpretations of soil drainage conditions. Soil Sci. Soc. Am. Proc. 37:413–412.
Bosch, D.D., and L.T. West. 1998. Hydraulic conductivity for two sandy soils. Soil Sci. Soc. Am. J. 62:90–98.
Cambardella, C.A., T.B. Moorman, T.B. Parkin, D.L. Karlen, R.F. Turco, and A.E. Konopka. 1994. Field scale variability of soil properties in Central Iowa soils. Soil Sci. Soc. Am. J. 58:1501–1511.
Cameron, D.R. 1978. Variability of soil water retention curves and predicted hydraulic conductivities on a small plot. Soil Sci. 126:364–371.
Campbell, J.B. 1978. Spatial variation of sand content and pH within single contiguous delineations of two soil mapping units. Soil Sci. Soc. Am. J. 39:460–464.
Clark, I. 1979. Practical geostatistics. Applied Sci. Publ., London.
Cliff, A.D., and J.K. Ord. 1973. Spatial autocorrelation. Pion, London.
David, M. 1977. Geostatistics area reserve estimation. Elsevier Sci. Publ., Amsterdam.
Gajem, Y.M., A.W. Warrick, and D.E. Myers. 1981. Spatial structure of soil physical properties of a Typic Torrifluvent soil. Soil Sci. Soc. Am. J. 45:709–715.
Gee, G.W., and J.W. Bauder. 1986. Particle size analysis. p. 404–407. In A. Klute (ed.) Methods of soil analysis. Part 1. 2nd ed. Agron. Monogr. 9. ASA and SSSA, Madison, WI.
Goovaerts, P. 1997. Geostatistics for natural resources evaluation. Oxford Univ. Press, New York.
Haan, C.T. 1997. Statistical methods in hydrology. Iowa State Univ. Press, Ames.
Heiskanen, J., and K. Makitalo. 2002. Soil water retention characteristics of Scots pine and Norway spruce forest sites in Finnish Lapland. For. Ecol. Manage. 162:137–152.
Journel, A.G., and C.J. Huijbregts. 1978. Mining geostatistics. Academic Press, London.
Jury, W.A., W.R. Gardner, and W.H. Gardner. 1991. Soil physics. 5th ed. John Wiley & Sons, New York.
Klute, A. 1986. Water retention: Laboratory methods. p. 635–662. In A. Klute (ed.) Methods of soil analysis. Part 1. 2nd ed. Agron. Monogr. 9. ASA and SSSA, Madison, WI.
Klute, A., and C. Dirksen. 1986. Hydraulic conductivity and diffusivity: Laboratory methods. p. 687–734. In A. Klute (ed.) Methods of soil analysis. Part 1. 2nd ed. Agron. Monogr. 9. ASA and SSSA, Madison, WI.
Logan, W.N. 1916. The soils of Mississippi. Tech. Bull. No. 7. Miss. Agric. Exp. Stn., Mississippi State Univ., Mississippi State.
McBratney, A.B., and M.J. Pringle. 1999. Estimating average and proportional variograms of soil properties and their potential use in precision agriculture. Precis. Agric. 1:219–236.
Mckinion, J.M., J.N. Jenkins, D. Akins, S.B. Turner, J.L. Willers, E. Jallas, and F.D. Whisler. 2001. Analysis of a precision agriculture approach to cotton production. Comput. Electron. Agric. 32:213–228.
Moran, P.A. 1950. Notes on continuous stochastic phenomena. Biometrika 37:17–23.
Rabenhorst, M.C. 1988. Determination of organic carbon and carbonate carbon in calcareous soils using dry combustion. Soil Sci. Soc. Am. J. 52:965–969.
Rasse, D.P., A.J.M. Smucker, and D. Santos. 2000. Alfalfa root and shoot mulching effects on soil hydraulic properties and aggregation. Soil Sci. Soc. Am. J. 64:725–731.
SAS Institute. 1996. SAS systems for information delivery for Windows. Release 6.12. SAS Inst., Cary, NC.
Shapiro, S.S., and M.B. Wilk. 1965. An analysis of variance test for normality. Biometrika 52:691–710.
S-Plus. 1997. S+ SpatialStats user's manual for Windows and Unix. Data Analysis Product Division, MathSoft, Seattle, WA.
Sobieraj, J.A., H. Elsenbeer, and G. Cameron. 2003. Scale dependency in spatial patterns of saturated hydraulic conductivity. Catena 55:49–77.
Stockton, J.G., and A.W. Warrick. 1971. Spatial variability of unsaturated hydraulic conductivity. Soil Sci. Soc. Am. Proc. 35:847–848.
Trangmar, B.B., R.S. Yost, and G. Uehara. 1985. Application of geostatistics to spatial studies of soil properties. Adv. Agron. 38:45–93.
Tsegaye, T., and R.L. Hill. 1998. Intensive tillage effects on spatial variability of soil physical properties. Soil Sci. 163:143–154.
USDA-NRCS. 1951. Bolivar County Mississippi. USDA-NRCS Publ. no. 5. U.S. Gov. Print. Office, Washington, DC.
Vauclin, M., S.R. Viera, G. Vachaud, and D.R. Nielsen. 1983. The use of co-kriging with limited field soil observations. Soil Sci. Soc. Am. J. 47:175–184.
Vieira, S.R., D.R. Nielsen, and J.W. Biggar. 1981. Spatial variability of field-measured infiltration rate. Soil Sci. Soc. Am. J. 45:1040–1048.
Webster, R. 1973. Automatic soil boundary location from transect data. Math. Geol. 5:27–37.
Webster, R., and H.E. Cuanalo De La C. 1975. Soil transect correlograms of north Oxfordshire and their interpretations. J. Soil Sci. 26:176–194.